SCIENCE CHINA
Information Sciences

• RESEARCH PAPER •
Special Focus on Advanced Nonlinear Control of Hypersonic Flight Vehicles

July 2015, Vol. 58 070205:1–070205:15
doi: 10.1007/s11432-015-5349-z

Adaptive mode switching of hypersonic morphing aircraft based on type-2 TSK fuzzy sliding mode control

JIAO Xin[1], FIDAN Baris[2], JIANG Ju[1]* & KAMEL Mohamed[2]

[1]*Nanjing University of Aeronautics and Astronautics, Nanjing* 210016*, China;*
[2]*University of Waterloo, Waterloo* N2L 3G1*, Canada*

Received November 13, 2014; accepted February 10, 2015; published online June 2, 2015

Abstract This paper presents a novel adaptive mode switching scheme for hypersonic morphing aircraft with retracted winglets based on type-2 Takagi-Sugeno-Kang (TSK) fuzzy sliding mode control. For each of retracting and stretching modes, a specific sliding mode controller has been adopted. Drawing upon input/output linearization to globally linearize the nonlinear model of the hypersonic aircraft at first, a type-2 TSK fuzzy logic system is devised for robust mode switching between these sliding mode controllers. For rapid stabilization of the system, the adaptive law for mode switching is designed using a direct constructive Lyapunov analysis. Simulation results demonstrate the stability and smooth transition using the proposed switched control scheme.

Keywords hypersonic morphing aircraft, mode switching, type-2 TSK fuzzy logic system, adaptive control, sliding mode control

Citation Jiao X, Fidan B, Jiang J, et al. Adaptive mode switching of hypersonic morphing aircraft based on type-2 TSK fuzzy sliding mode control. Sci China Inf Sci, 2015, 58: 070205(15), doi: 10.1007/s11432-015-5349-z

1 Introduction

Hypersonic morphing aircraft (HMA) [1] refers to hypersonic aircraft with variable wings to accomplish specific tasks better. The HMA has the same characteristics as other hypersonic aircraft, including rapid time-variation, strong nonlinearity, strong coupling, and model uncertainty [2,3], which cause difficulty in designing flight controller. In practice, hypersonic aircraft always fly within a large flight condition range, which causes frequent switching of the conditions [4]. The controller that keeps stabilization around a single nominal flight condition cannot be used any more. Complex nonlinear systems cannot be controlled easily in the switching process by simple control methods, which increase the difficulty of flight control for hypersonic aircraft [5–7].

An HMA with retracted winglets needs to retract or stretch its winglets in large flight envelopes. If the switching control cannot overcome the state saltation phenomenon while switching the modes of winglets, it is hard to keep the process of retracting or stretching winglets smooth and stable [8,9]. Our purpose is to construct an appropriate control of mode switching to keep the switching processes smooth and stable.

* Corresponding author (email: jiangju@nuaa.edu.cn)

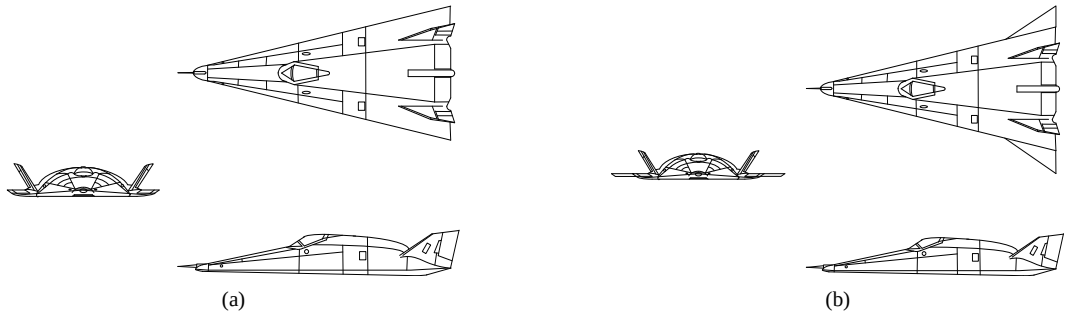

Figure 1 An illustration of a typical HMA's modes based on X-24B configuration. (a) The three views of vehicle in retracting mode; (b) the three views of vehicle in stretching mode. Modified from [24].

In nonlinear control designs for hypersonic aircraft, sliding mode control (SMC) has been widely used. The SMC provides a systematic approach to the problem of maintaining stability and consistent performance in the face of modeling imprecision. For example, terminal SMC was combined with a second-order SMC approach to solve the parameter uncertainties of a hypersonic vehicle in [10,11]. A continuous high order sliding mode controller was designed to reject aerodynamic uncertainties in [12,13]. The main advantage of the SMC is that system response remains insensitive to model uncertainties and disturbances. However, chattering phenomenon is the key drawback involved by using pure SMC [14]. Therefore, SMC is always combined with some filtering and fine-tuning methods for real-life applications.

In switching processes, the factors of uncertainties, such as disturbance, have to be overcome. Interval type-2 TSK fuzzy approach [15,16], has been proven to overcome such factors in various problems [17,18] and has been increasingly used in control of uncertain systems. Traditional type-1 TSK fuzzy logic systems [19–21] have been used to solve such control problems [22,23]; however, as systems become more complex, the exact fuzzy sets and membership functions are no longer enough to accomplish the task. Thus, the type-2 fuzzy logic controller has arisen and undergone rapid development because of its ability to deal with problems of uncertainty more effectively. Moreover, the control format of mode switching is similar to the type-2 TSK fuzzy tools. Considering the advantages of SMC of nonlinear systems and the characteristics of type-2 TSK fuzzy techniques, a type-2 TSK fuzzy switching scheme combined with SMC is proposed for adaptive control of HMA in this paper.

The outline of the paper is as follows. Section 2 presents the model of HMA and gives the aerodynamic parameters of vehicle in retracting, stretching and switching modes. In Section 3, the switching mechanism is discussed first, and afterwards, the novel switching control is designed by combining type-2 TSK fuzzy and SMC. Moreover, the adaptive signals are obtained drawing upon a direct constructive Lyapunov analysis. In Section 4, we conduct two simulation studies to test and verify the effectiveness of the switching control. Finally, conclusions are presented in Section 5.

2 Model of hypersonic morphing aircraft

A hypersonic flight vehicle with retracted winglets is researched in this paper. The data comes from an experimental aircraft model. The only difference between retracting mode and stretching mode is the mode of the winglets which are used to adjust the lift-drag ratio, mean aerodynamic chord and reference area. Illustrations of typical HMA retracting and stretching winglet modes based on X-24B configuration [24] are shown in Figure 1.

According to the longitudinal force and moment equilibrium, the longitudinal dynamics model of HMA [25] can be obtained as follows.

$$\dot{V} = \frac{T\cos\alpha - D}{m} - \frac{\mu\sin\gamma}{r^2}, \tag{1}$$

$$\dot{\gamma} = \frac{L + T\sin\alpha}{mV} - \frac{\left(\mu - V^2 r\right)\cos\gamma}{Vr^2}, \tag{2}$$

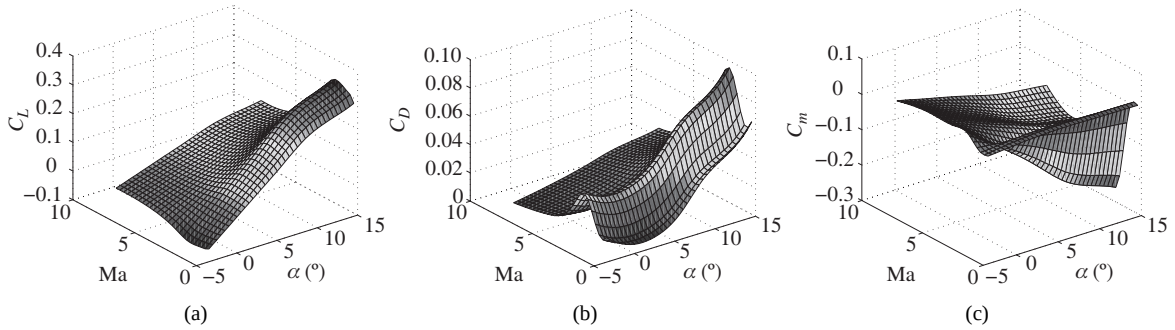

Figure 2 The aerodynamic parameters of vehicle in retracting mode. (a) The lift coefficient; (b) the drag coefficient; (c) the pitch moment coefficient.

$$\dot{q} = \frac{M_y}{I_y}, \tag{3}$$

$$\dot{\alpha} = q - \dot{\gamma} \tag{4}$$

$$\dot{h} = V \sin\gamma, \tag{5}$$

$$\ddot{\beta} = -2\xi\omega\dot{\beta} - \omega^2\beta + \omega^2\beta_c. \tag{6}$$

In this model, V, γ, q, α, h are the velocity, flight path angle, pitch rate, angle of attack, and altitude, respectively; β, ω, ξ are the throttle setting, natural frequency, and damping coefficient, respectively; m, μ, r, M_y, I_y are the mass, gravitational constant, radial distance from the earth's center, pitching moment, and moment of inertia, respectively. For the lift L, drag D, thrust T, we have

$$L = \frac{1}{2}\rho V^2 s C_L, \tag{7}$$

$$D = \frac{1}{2}\rho V^2 s C_D, \tag{8}$$

$$T = \frac{1}{2}\rho V^2 s C_T, \tag{9}$$

$$C_m(\delta_e) = 0.0292(\delta_e - \alpha), \tag{10}$$

$$M = \frac{1}{2}\rho V^2 s\bar{c}\left(C_m + C_m(\delta_e)\right), \tag{11}$$

$$C_T = \begin{cases} 0.02576\beta, & \text{if } \beta < 1, \\ 0.0224 + 0.00336\beta, & \text{if } \beta \geqslant 1, \end{cases} \tag{12}$$

where C_L, C_D, C_T, C_m are lift, drag, thrust and pitch moment coefficients respectively; ρ, s, R_e are the density of the air, reference area, and radius of the earth, respectively. The applicable control signals are the throttle setting command β_c in (6) and the elevator angle δ_e in (11). The specific dynamic coefficients are from a set of experimental data. Based on the same data set, we have $m = 136820$ kg, $I_y = 9490740\ \text{kg}\cdot\text{m}^2$.

In the retracting mode, $s = 369\ \text{m}^2$, $\bar{c} = 27$ m, the aerodynamic parameters of lift, drag and pitch moment coefficients for different Mach and angle of attack values are shown in Figure 2.

In the stretching mode, $s = 389\ \text{m}^2$, $\bar{c} = 30$ m, the aerodynamic parameters of lift, drag and pitch moment coefficient for different Mach and angle of attack values are shown in Figure 3.

We consider a flight scenario where the aircraft is in retracting mode before time instant t_1, then we would like to morph the aircraft within the time interval $[t_1, t_2]$, so that it completely switches to stretching mode after time instant t_2.

Assumption 1. Any system parameter $X(t)$, including s, $\bar{c}$, and all the aerodynamic parameters, is switched.

$$X(t) = X_1(t)\mathrm{e}^{(-a(t-t_1))} + X_2(t)\left(1 - \mathrm{e}^{(-a(t-t_1))}\right), \tag{13}$$

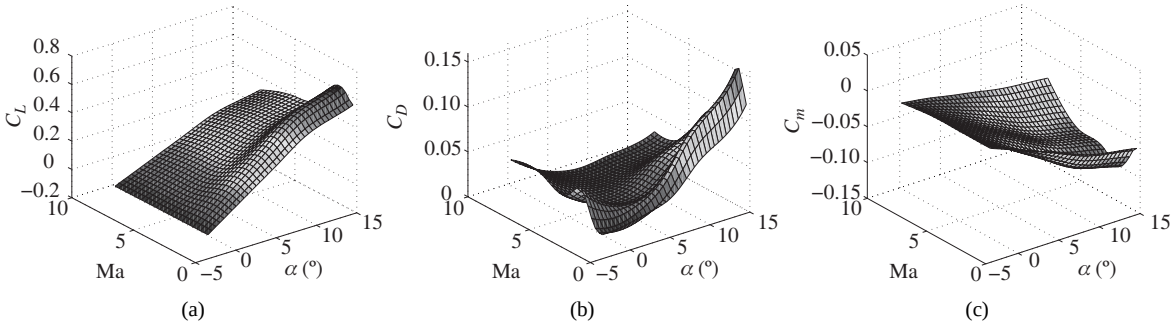

Figure 3 The aerodynamic parameters of vehicle in stretching mode. (a) The lift coefficient; (b) the drag coefficient; (c) the pitch moment coefficient.

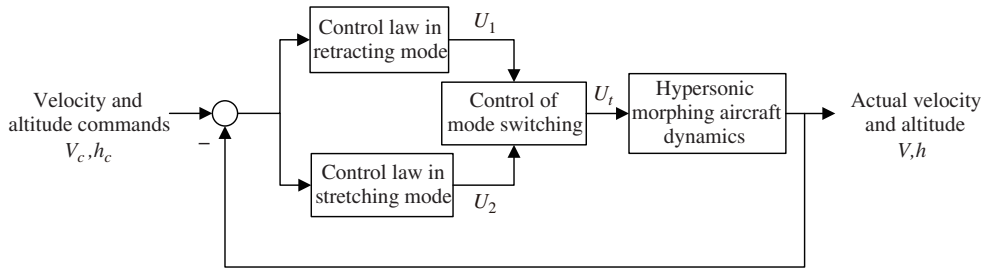

Figure 4 The system structure of switching control.

where X_1 stands for value in retracting mode, X_2 stands for value in stretching mode, X stands for value in switching mode. When $t = t_1$, s, $\bar{c}$, and all the aerodynamic parameters are retracting mode values. When $t_1 < t \leqslant t_2$, s, $\bar{c}$, the weights of values in retracting mode decrease while the weights of values in stretching mode increase gradually, and eventually, at $t = t_2$, the stretching mode values are reached.

Consequently, in terms of the aerodynamic parameters in retracting mode and stretching mode, we can obtain the aerodynamic parameters in switching process.

3 Design of adaptive switching control

We consider the problem of tracking desired velocity and altitude trajectories V_c and h_c for the HMA described in Section 2. In the literature, there are control design studies for such problem for the case of fixed structure aircraft. Our focus is to perform the task for the HMA, robustly to the abrupt changes in the aircraft dynamics due to mode switching. In the problem, similar to the relevant studies in the literature, we assume that the flight state $x = [V,\ \gamma,\ \alpha,\ \beta,\ h]^{\mathrm{T}}$ is available for measurement.

Define $U_1 = [\beta_{c1}, \delta_{e1}]^{\mathrm{T}}$ as the control signal of retracting mode and $U_2 = [\beta_{c2}, \delta_{e2}]^{\mathrm{T}}$ as the control signal of stretching mode. When the HMA switches the mode of winglets, the control signal has to be switched correspondingly. The control of switching process is as follows.

$$U(t) = \begin{cases} U_1(t), & t \leqslant t_1, \\ U_t(t), & t_1 < t \leqslant t_2, \\ U_2(t), & t > t_2, \end{cases} \tag{14}$$

where $U_t = [\beta_{ct}, \delta_{et}]^{\mathrm{T}}$ is the control signal of mode switching, which can be expressed as follows.

$$U_t = \begin{bmatrix} \beta_{ct}(t) \\ \delta_{et}(t) \end{bmatrix} = \begin{bmatrix} a_\beta(t)\beta_{c1}(t) \\ a_\delta(t)\delta_{e1}(t) \end{bmatrix} + \begin{bmatrix} b_\beta(t)\beta_{c2}(t) \\ b_\delta(t)\delta_{e2}(t) \end{bmatrix}, \tag{15}$$

where a_β, a_δ, b_β, b_δ are the time varying control signal weights to be produced by the switching scheme.

The system structure of the switching control is shown in Figure 4.

3.1 Sliding mode control in retracting mode and stretching mode

3.1.1 *Input/Output feedback linearization*

For the longitudinal nonlinear model of hypersonic aircraft (1)–(5), the third derivative of V and the fourth derivative of h are obtained as follows [2,3].

$$\begin{cases} \dot{V} = \dfrac{T\cos\alpha - D}{m} - \dfrac{\mu\sin\gamma}{r^2} = f_1(x), \\ \ddot{V} = \dfrac{\partial f_1(x)}{\partial x}\dot{x} = \omega_1\dot{x}, \\ \dddot{V} = \dot{x}^{\mathrm{T}}\dfrac{\partial\omega_1}{\partial x}\dot{x} + \omega_1\ddot{x} = \omega_1\ddot{x} + \dot{x}^{\mathrm{T}}\omega_2\dot{x}, \end{cases} \tag{16}$$

$$\begin{cases} \dot{h} = V\sin\gamma, \\ \ddot{h} = \dot{V}\sin\gamma + V\dot{\gamma}\cos\gamma, \\ \dddot{h} = \ddot{V}\sin\gamma + 2\dot{V}\dot{\gamma}\cos\gamma - V\dot{\gamma}^2\sin\gamma + V\ddot{\gamma}\cos\gamma, \\ h^{(4)} = \dddot{V}\sin\gamma + 3\ddot{V}\dot{\gamma}\cos\gamma - 3\dot{V}\gamma^2\sin\gamma + 3\dot{V}\ddot{\gamma}\cos\gamma - V\dot{\gamma}^3\cos\gamma - 3V\dot{\gamma}\ddot{\gamma}\sin\gamma + V\cos\gamma\cdot\dddot{\gamma}, \end{cases} \tag{17}$$

where the first, second and third derivatives of γ are obtained according to (2) as

$$\begin{cases} \dot{\gamma} = \dfrac{L + T\sin\alpha}{mV} - \dfrac{\left(\mu - V^2 r\right)\cos\gamma}{Vr^2} = f_2(x), \\ \ddot{\gamma} = \dfrac{\partial f_2(x)}{x}\dot{x} = \pi_1\dot{x}, \\ \dddot{\gamma} = \dot{x}^{\mathrm{T}}\dfrac{\partial\pi_1}{\partial x}\dot{x} + \pi_1\ddot{x} = \pi_1\ddot{x} + \dot{x}^{\mathrm{T}}\pi_2\dot{x}. \end{cases} \tag{18}$$

Note again that, in (16) and (18), the flight state vector $x = [V,\ \gamma,\ \alpha,\ \beta,\ h]^{\mathrm{T}}$ is available for measurement, $\omega_1 = \partial f_1(x)/\partial x$, $\omega_2 = \partial\omega_1/\partial x$, $\pi_1 = \partial f_2(x)/\partial x$, $\pi_2 = \partial\pi_1/\partial x$. The linearized model is obtained as follows.

$$\begin{bmatrix} \dddot{V} \\ h^{(4)} \end{bmatrix} = \begin{bmatrix} f_V \\ f_h \end{bmatrix} + \begin{bmatrix} b_{11} & b_{12} \\ b_{21} & b_{22} \end{bmatrix} \begin{bmatrix} \beta_c \\ \delta_e \end{bmatrix}, \tag{19}$$

where

$$f_V = \left(\omega_1\ddot{x}_0 + \dot{x}\omega_2\dot{x}\right)/m, \tag{20}$$

$$f_h = 3\ddot{V}\dot{\gamma}\cos\gamma - 3\dot{V}\dot{\gamma}^2\sin\gamma + 3\dot{V}\ddot{\gamma}\cos\gamma - 3V\dot{\gamma}\ddot{\gamma}\sin\gamma - V\dot{\gamma}^3\cos\gamma + \left(\omega_1\ddot{x}_0 + \dot{x}^{\mathrm{T}}\omega_2\dot{x}\right)\sin\gamma/m + V\cos\gamma\left(\pi_1\ddot{x}_0 + \dot{x}^{\mathrm{T}}\pi_2\dot{x}\right), \tag{21}$$

$$b_{11} = \frac{\rho V^2 s\cdot C_\beta\omega^2}{2m}\cos\alpha, \tag{22}$$

$$b_{12} = -\frac{\rho V^2 s\bar{c}\cdot c_e}{2mI_y}(T\sin\alpha + D_\alpha), \tag{23}$$

$$b_{21} = \frac{\rho V^2 s C_\beta\omega^2}{2m}\sin(\alpha+\gamma), \tag{24}$$

$$b_{22} = \frac{\rho V^2 s\bar{c}\cdot c_e}{2mI_y}\left[T\cos(\alpha+\gamma) + L_\alpha\cos\gamma - D_\alpha\sin\gamma\right]. \tag{25}$$

3.1.2 *Sliding mode control*

We first consider a pair of SMC designs, one for each of the retracting and the stretching modes, considering the nominal system parameters for that mode.

In the SMC design, following Lyapunov approach, we aim to satisfy the condition $S\dot{S} < 0$ to have an appropriate sliding mode selection S converge to zero. Similar to [3], we define the sliding mode surfaces as

$$\begin{cases} S_V = (d/dt + \lambda_V)^2 e_V(t) = \ddot{V} - \ddot{V}_d + 2\lambda_V \dot{e}_V + \lambda_V^2 e_V, \\ S_h = (d/dt + \lambda_h)^3 e_h(t) = \dddot{h} - \dddot{h}_d + 3\lambda_h \ddot{e}_h + 3\lambda_h^2 \dot{e}_h + \lambda_h^3 e_h. \end{cases} \tag{26}$$

Then, the derivatives of S_V and S_h are obtained as

$$\begin{cases} \dot{S}_V = \dddot{V} - \dddot{V}_d + 2\lambda_V \ddot{e}_V + \lambda_V^2 \dot{e}_V, \\ \dot{S}_h = h^{(4)} - h_d^{(4)} + 3\lambda_h \dddot{e}_h + 3\lambda_h^2 \ddot{e}_h + \lambda_h^3 \dot{e}_h. \end{cases} \tag{27}$$

In order to avoid chattering phenomenon, we choose the saturation SMC laws

$$\begin{cases} \dot{S}_V = -k_V \mathrm{sat}(S_V), \\ \dot{S}_h = -k_h \mathrm{sat}(S_h), \end{cases} \tag{28}$$

where k_V, k_h are positive integers, $\mathrm{sat}(S_V)$ and $\mathrm{sat}(S_h)$ are saturation functions, defined as $\mathrm{sat}(x) = x$ if $|x| \leqslant 1$ and $\mathrm{sat}(x) = \mathrm{sgn}(x)$ otherwise. Then, we can get: $S_V \dot{S}_V < 0$, $S_h \dot{S}_h < 0$, which satisfy the sliding condition. Accordingly, the control signal can be obtained as follows.

$$U = \begin{bmatrix} \beta_c \\ \delta_e \end{bmatrix} = \begin{bmatrix} b_{11} & b_{12} \\ b_{21} & b_{22} \end{bmatrix}^{-1} \cdot \begin{bmatrix} \dddot{V}_d - f_V - 2\lambda_V \ddot{e}_V - \lambda_V^2 \dot{e}_V - k_V \mathrm{sat}(S_V) \\ h_d^{(4)} - f_h - 3\lambda_h \dddot{e}_h - 3\lambda_h^2 - \lambda_h^3 \dot{e}_h - k_h \mathrm{sat}(S_h) \end{bmatrix}. \tag{29}$$

Note that in (29), b_{ij}, f_V, f_h terms depend on flight conditions. Hence, even if the coefficients λ_V, λ_h are selected the same, the control law (29) will have different coefficients in retracting and stretching modes, depending on the values of b_{ij}, f_V, f_h in each of these two modes.

3.2 Adaptive mode switching based on type-2 TSK fuzzy sliding mode control

Each of the two SMC laws designed based on the procedure in Subsection 3.1 is valid only for the corresponding mode. Due to nonlinearity and parametric sensitivity of the model, using a single fixed SMC law for both modes will not meet the tracking control requirements. To solve this issue by switching the SMC law from one mode to the other robustly, an adaptive mode switching scheme based on type-2 TSK fuzzy technique is proposed. The structure is shown in Figure 5: (a) depicts the overall adaptive control scheme based on the type-2 fuzzy logic system with diagram shown in (b). A similar type-2 fuzzy logic system was used in [26].

In Figure 5, the control signals U_1, U_2 are the inputs of the type-2 TSK fuzzy logic controller. After fuzzy reasoning, type reducer and defuzzication, the crisp output of type-2 TSK fuzzy logic controller can be obtained. For keeping robustness of controller, the compensation law is used to compensate the difference between the output of type-2 TSK fuzzy logic controller and the desired solution of control signal. The estimator is used to estimate some variables of compensation law. The adaptive law is obtained, following a constructive Lyapunov analysis, as detailed in the sequel.

3.2.1 *Type-2 TSK fuzzy logic system*

The traditional fuzzy systems based on type-1 fuzzy set has limitation to deal with the uncertainties of practical plants. In order to enhance the traditional fuzzy system capability of describing and handling uncertainties, type-2 TSK fuzzy logic approach based on type-2 fuzzy sets is utilized in this paper. For the block of type-2 TSK fuzzy logic shown in Figure 5(a), U_1, U_2 are the inputs and U_f is the output. The structure of type-2 fuzzy logic system [27,28] is shown in Figure 5(b).

In this paper, we use the Gaussian primary membership function with uncertain mean as the input membership function and the output membership function.

Define:

$$U_b(t) = [\mathrm{diag}(U_1(t)), \mathrm{diag}(U_2(t))] = \begin{bmatrix} \beta_{c1}(t) & 0 & \beta_{c2}(t) & 0 \\ 0 & \delta_{e1}(t) & 0 & \delta_{e2}(t) \end{bmatrix}. \tag{30}$$

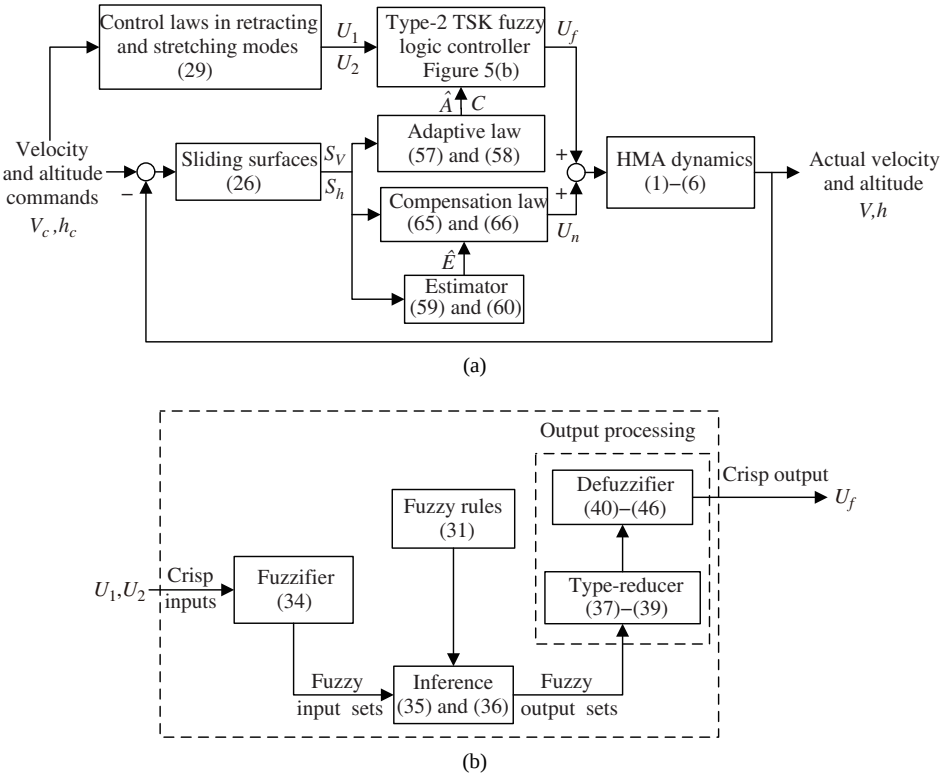

Figure 5 Block diagram of the closed loop system using the proposed type-2 fuzzy logic base adaptive switching controller. (a) The system structure of adaptive switching control; (b) the structure of type-2 fuzzy logic system.

We describe the ith-rule of interval type-2 TSK fuzzy logic system (A2-C0 case) as

$$\text{Rule } j: \text{ If } U_1(t) \in \tilde{F}_1^j, \text{and } U_2(t) \in \tilde{F}_2^j, \text{ then } U_f(t) = U_f^j(t) = U_b(t)C^j, \tag{31}$$

where $U_1(t)$ is the control signal of retracting mode, $U_2(t)$ is the control signal of stretching mode; $\tilde{F}_1^j$ is the interval type-2 fuzzy set of $U_1(t)$, $\tilde{F}_2^j$ is the interval type-2 fuzzy set of $U_2(t)$; $U_f(t)$ stands for output of type-2 TSK fuzzy; $C^j = [c_1^j, c_2^j]^{\mathrm{T}}$, $c_1^j = [c_{\beta_c 1}^j, c_{\delta_e 1}^j]$, $c_2^j = [c_{\beta_c 2}^j, c_{\delta_e 2}^j]$ are consequent parameters, what we want to design as the solutions of a_β, a_δ, b_β, b_δ in (15) to obtain the control signal of mode switching.

The type-2 TSK fuzzy sets $\tilde{F}_1^j$ and $\tilde{F}_2^j$ are characterized by type-2 membership function $\mu_{\tilde{F}_1^j}$ and $\mu_{\tilde{F}_2^j}$ respectively.

Suppose that $\underline{\mu}_{\tilde{F}_i^j}$ and $\bar{\mu}_{\tilde{F}_i^j}$ are lower membership function and upper membership function of $\mu_{\tilde{F}_i^j}$ $(i = 1, 2)$, respectively. $N(m, \sigma)$ is the normal distribution with mean m and variance σ. The upper membership function $\bar{\mu}_{\tilde{F}_i^j}(U_i(t))$ is given by

$$\bar{\mu}_{\tilde{F}_i^j}(U_i(t)) = \begin{cases} N\big(m_{i1}^j, \sigma_i^j\big), & U_i < m_{i1}^j, \\ 1, & m_{i1}^j \leqslant U_i \leqslant m_{i2}^j, \\ N\big(m_{i2}^j, \sigma_i^j\big), & U_i > m_{i2}^j, \end{cases} \tag{32}$$

and the lower membership function $\underline{\mu}_{\tilde{F}_i^j}(U_i(t))$ is given by

$$\underline{\mu}_{\tilde{F}_i^j}(U_i(t)) = \begin{cases} N\big(m_{i2}^j, \sigma_i^j\big), & U_i \leqslant (m_{i1}^j + m_{i2}^j)/2, \\ N\big(m_{i1}^j, \sigma_i^j\big), & U_i > (m_{i1}^j + m_{i2}^j)/2. \end{cases} \tag{33}$$

Consequently, the membership function which is an interval with lower and upper boundaries is

$$\mu_{\tilde{F}_i^j}(U_i(t)) = \left[\underline{\mu}_{\tilde{F}_i^j}(U_i(t)), \bar{\mu}_{\tilde{F}_i^j}(U_i(t))\right]. \tag{34}$$

In the type-2 TSK fuzzy logic system we used interval type-2 fuzzy sets and "meet" operation under product t-norm, so the result of the input and antecedent operations, which are contained in the firing set $\prod_{i=1}^{2}\mu_{\tilde{F}_i^j}(U_i(t)) \equiv F^j(U_i(t))$, is an interval type-1 set [29].

$$F^j(t) = \left[\underline{f}^j(U(t)), \bar{f}^j(U(t))\right] = \left[\underline{f}^j(t), \bar{f}^j(t)\right], \tag{35}$$

where

$$\begin{cases} \underline{f}^j(t) = \underline{\mu}_{\tilde{F}_1^j}(U_1(t)) * \underline{\mu}_{\tilde{F}_2^j}(U_2(t)), \\ \bar{f}^j(t) = \bar{\mu}_{\tilde{F}_1^j}(U_1(t)) * \bar{\mu}_{\tilde{F}_2^j}(U_2(t)). \end{cases} \tag{36}$$

The type reducer is used to generate a type-1 fuzzy set output, which is also an interval set. We used center of sets (cos) type reduction, which is expressed as

$$\begin{aligned} U_{fcos}(t) &= [U_{fl}(t), U_{fr}(t)] \\ &= \int_{U_f^1 \in [U_{fl}^1, U_{fr}^1]} \cdots \int_{U_f^M \in [U_{fl}^M, U_{fr}^M]} \int_{f^1 \in [\underline{f}^1, \bar{f}^1]} \cdots \int_{f^M \in [\underline{f}^M, \bar{f}^M]} 1 \Big/ \frac{\sum_{j=1}^{M} f^j(t) U_f^j(t)}{\sum_{j=1}^{M} f^j(t)}, \end{aligned} \tag{37}$$

where $U_{fcos}(t)$ is the interval set; $U_{fl}(t)$ is the left-most point of $U_f(t)$, $U_{fr}(t)$ is the right-most point of $U_f(t)$. M is the number of type-2 fuzzy rules. Then we have

$$\begin{aligned} U_{fr}(t) &= U_{fr}(t)\left(\underline{f}^1, \ldots, \underline{f}^R, \bar{f}^{R+1}, \ldots, \bar{f}^M, U_f^1, \ldots, U_f^M\right) \\ &= \frac{\sum_{j=1}^{R} \underline{f}^j(t) U_f^j(t) + \sum_{j=R+1}^{M} \bar{f}^j(t) U_f^j(t)}{\sum_{j=1}^{R} \underline{f}^j(t) + \sum_{j=R+1}^{M} \bar{f}^j(t)}, \end{aligned} \tag{38}$$

$$\begin{aligned} U_{fl}(t) &= U_{fl}(t)\left(\bar{f}^1, \ldots, \bar{f}^L, \underline{f}^{L+1}, \ldots, \underline{f}^M, U_f^1, \ldots, U_f^M\right) \\ &= \frac{\sum_{j=1}^{L} \bar{f}^j(t) U_f^j(t) + \sum_{j=L+1}^{M} \underline{f}^j(t) U_f^j(t)}{\sum_{j=1}^{L} \bar{f}^j(t) + \sum_{j=L+1}^{M} \underline{f}^j(t)}, \end{aligned} \tag{39}$$

where L and R are the numbers of points which separate $U_{fl}(t)$ and $U_{fr}(t)$ into two sides respectively, one side using lower firing strengths and the other using upper firing strengths.

Consequently, the de-fuzzified crisp output $U_f(t)$ is

$$\begin{aligned} U_f(t) &= (U_{fl}(t) + U_{fr}(t))/\,2 \\ &= \frac{1}{2}\left(\frac{\sum_{j=1}^{L} \bar{f}^j(t) U_f^j(t) + \sum_{j=L+1}^{M} \underline{f}^i(t) U_f^j(t)}{\sum_{j=1}^{L} \bar{f}^j(t) + \sum_{j=L+1}^{M} \underline{f}^j(t)} + \frac{\sum_{j=1}^{R} \underline{f}^j(t) U_f^j(t) + \sum_{j=R+1}^{M} \bar{f}^j(t) U_f^j(t)}{\sum_{j=1}^{R} \underline{f}^j(t) + \sum_{j=R+1}^{M} \bar{f}^j(t)}\right), \end{aligned} \tag{40}$$

where $\underline{f}^j(t)$ and $\bar{f}^j(t)$ stand for the lower and upper membership functions of $\tilde{F}^j(t)$, respectively. Then the output of type-2 TSK fuzzy logic system in (40) can be rewritten as follows.

$$U_f(t) = \frac{1}{2}\left(\sum_{j=1}^{M} U_f^j(t)\xi_l^j(t) + \sum_{j=1}^{M} U_f^j(t)\xi_r^j(t)\right) = \frac{1}{2}\left(U_{fb}^{\mathrm{T}}(t)\xi_l(t) + U_{fb}^{\mathrm{T}}(t)\xi_r(t)\right) = U_{fb}^{\mathrm{T}}(t)\xi(t), \tag{41}$$

where $U_{fb}(t) = [U_f^1(t), U_f^2(t), \ldots, U_f^M(t)]^{\mathrm{T}}$, $\xi(t) = \frac{1}{2}(\xi_l(t) + \xi_r(t)) \equiv \xi(U_b(t))$, and

$$\xi_l^j(t) = \frac{h_l^j(t)}{\sum_{j=1}^{L} \bar{f}^j(t) + \sum_{j=L+1}^{M} \underline{f}^j(t)}, \tag{42}$$

$$\xi_r^j(t) = \frac{h_r^j(t)}{\sum_{j=1}^{R} \bar{f}^j(t) + \sum_{j=R+1}^{M} \underline{f}^j(t)}, \tag{43}$$

in which, M is the number of type-2 fuzzy rules, and there are

$$h_l^j(t) = \begin{cases} \bar{f}^j(t), & j = 1, \ldots, L, \\ \underline{f}^j(t), & j = L+1, \ldots, M, \end{cases} \tag{44}$$

$$h_r^j(t) = \begin{cases} \bar{f}^j(t), & j = 1, \ldots, R, \\ \underline{f}^j(t), & j = R+1, \ldots, M. \end{cases} \tag{45}$$

Remark: Note above that $U_{fb}(t) = [U_f^1(t), \ldots, U_f^M(t)]^{\mathrm{T}} = [C^1, \ldots, C^M]^{\mathrm{T}} U_b^{\mathrm{T}}(t) \triangleq C^{\mathrm{T}} U_b^{\mathrm{T}}(t)$. Hence, Eq. (41) can be rewritten as

$$U_f(t) = U_b(t)\Xi(t), \Xi(t) = C\xi(t) \equiv C\xi(U_b(t)). \tag{46}$$

3.2.2 *Type-2 TSK fuzzy sliding mode control*

Consider the constructive SMC analysis in Subsection 3.1.2 and the resultant SMC law (29). As mentioned previously, Eq. (29) will guarantee convergence of V to V_d and h to h_d only for the specific flight condition. Its coefficients are selected for, depending on the values of b_{ij}, f_V, f_h terms at that flight condition.

For a flight scenario involving a switch between retracting and stretching modes of the HMA, we can consider an ideal or desired control law

$$U^*(t) = \begin{bmatrix} \beta_c^*(t) \\ \delta_e^*(t) \end{bmatrix} = U_b(t)\Xi^*(t) \equiv U^*\left(U_b(t)\right) \tag{47}$$

that has the same form as (29), but b_{11}, b_{12}, b_{21}, b_{22}, and the coefficients of f_V, f_h depend on flight condition, and hence is time-varying.

Due to insufficient flight data, uncertainties, and external disturbances, Eq. (47) cannot be directly produced during the mode switch. To make the problem tractable, we assume that (47) can be applied at the full retracting and the full stretching mode using the system parameter information for these modes. Our approach will focus on approximation of (47) during mode switch by the output $U_f(t) = [\beta_{\mathrm{cf}}(t), \delta_{\mathrm{ef}}(t)]^{\mathrm{T}}$ of type-2 TSK fuzzy control scheme.

According to the universal approximation theorem, since U^* and ξ are both considered as functions of U_b,

$$U^*(t) = A^{*\mathrm{T}}\xi(t) + \varepsilon(t), \tag{48}$$

where A^* is an ideal constant matrix, $\varepsilon(t)$ is the approximation error satisfying $|\varepsilon_i(t)| < E_i$ $(i = 1, 2)$ for any pre-set constant $E_i > 0$, provided that L, R, M are sufficiently large. Let $\hat{E}(t)$ be the estimate of E, whose adaptive law will be defined in the sequel, and

$$\bar{E}(t) = \hat{E}(t) - E, \tag{49}$$

where $\bar{E}(t) = \left[\bar{E}_{\beta_c}(t), \bar{E}_{\delta_e}(t)\right]$. E is constant, and hence $\dot{\bar{E}}(t) = \dot{\hat{E}}(t)$.

We will define another adaptive law to generate the estimate of $U_f^*(t) = A^{*\mathrm{T}}\xi(t)$ as

$$\hat{U}_f(t) = \left[\hat{\beta}_{\mathrm{cf}}(t), \hat{\delta}_{\mathrm{ef}}(t)\right]^{\mathrm{T}} = \hat{A}^{\mathrm{T}}(t)\xi(t). \tag{50}$$

Therefore, the adaptive switching control of type-2 TSK fuzzy SMC can be expressed as

$$U(t) = \hat{U}_f(t) + U_n(t), \tag{51}$$

where $\hat{U}_f(t)$, as the main control signal, is used to mimic the desired control signal $U^*(t)$; $U_n(t) = [\beta_{\mathrm{cn}}(t), \delta_{\mathrm{en}}(t)]^{\mathrm{T}}$ is used to compensate the difference between desired control signal and the output of type-2 TSK fuzzy SMC.

According to (48) and (50), $\bar{U}_f(t)$ is defined as

$$\bar{U}_f(t) = \hat{U}_f(t) - U^*(t) = \hat{U}_f(t) - U_f^*(t) - \varepsilon(t) = \bar{A}^{\mathrm{T}}(t)\xi(t) - \varepsilon(t), \tag{52}$$

where $\bar{A}(t) = \hat{A}(t) - A^* = \left[\bar{A}_{\beta_c}(t), \bar{A}_{\delta_e}(t)\right]$. A^* is constant, and hence $\dot{\bar{A}}(t) = \dot{\hat{A}}(t)$.

Therefore, Eq. (19) can be rewritten as

$$\begin{bmatrix} \dddot{V} \\ h^{(4)} \end{bmatrix} = \begin{bmatrix} f_V \\ f_h \end{bmatrix} + \begin{bmatrix} b_{11} & b_{12} \\ b_{21} & b_{22} \end{bmatrix} \begin{bmatrix} \hat{\beta}_{\mathrm{cf}} + \beta_{\mathrm{cn}} \\ \hat{\delta}_{\mathrm{ef}} + \delta_{\mathrm{en}} \end{bmatrix}. \tag{53}$$

From (27), (28), and (53), we obtain that:

$$\begin{bmatrix} \dot{S}_V \\ \dot{S}_h \end{bmatrix} = \begin{bmatrix} b_{11} & b_{12} \\ b_{21} & b_{22} \end{bmatrix} \begin{bmatrix} \hat{\beta}_{\mathrm{cf}} + \beta_{\mathrm{cn}} - \beta_c^* \\ \hat{\delta}_{\mathrm{ef}} + \delta_{\mathrm{en}} - \delta_e^* \end{bmatrix} - \begin{bmatrix} k_V \mathrm{sat}(S_V) \\ k_h \mathrm{sat}(S_h) \end{bmatrix}. \tag{54}$$

3.2.3 *Stability analysis and adaptive law design*

For the process of mode switching, in order to establish the stability of the closed loop system depicted in Figure 5, a Lyapunov stability analysis is adopted. To make the sliding mode variable S, $\bar{A}_{\beta_c}$, $\bar{A}_{\delta_e}$, $\bar{E}_{\beta_c}$ and $\bar{E}_{\delta_e}$ approach zero, we define the Lyapunov function as

$$V = \frac{1}{2}S^{\mathrm{T}}S + \frac{1}{2\eta_1}\bar{A}_{\beta_c}^{\mathrm{T}}\bar{A}_{\beta_c} + \frac{1}{2\eta_2}\bar{A}_{\delta_e}^{\mathrm{T}}\bar{A}_{\delta_e} + \frac{1}{2\eta_3}\bar{E}_{\beta_c}^{\mathrm{T}}\bar{E}_{\beta_c} + \frac{1}{2\eta_4}\bar{E}_{\delta_e}^{\mathrm{T}}\bar{E}_{\delta_e}, \tag{55}$$

where $S = [S_V, S_h]^{\mathrm{T}}$, $\bar{A} = \left[\bar{A}_{\beta_c}, \bar{A}_{\delta_e}\right]$, $\bar{E} = \left[\bar{E}_{\beta_c}, \bar{E}_{\delta_e}\right]^{\mathrm{T}}$, $\varepsilon = [\varepsilon_{\beta_c}, \varepsilon_{\delta_e}]^{\mathrm{T}}$, η_1, η_2, η_3, and η_4 are all positive constant. The derivative of (55) with respect to time is obtained as

$$\begin{aligned}
\dot{V} =\ & S^{\mathrm{T}}\dot{S} + \frac{1}{\eta_1}\bar{A}_{\beta_c}^{\mathrm{T}}\dot{\bar{A}}_{\beta_c} + \frac{1}{\eta_2}\bar{A}_{\delta_e}^{\mathrm{T}}\dot{\bar{A}}_{\delta_e} + \frac{1}{\eta_3}\bar{E}_{\beta_c}^{\mathrm{T}}\dot{\bar{E}}_{\beta_c} + \frac{1}{\eta_4}\bar{E}_{\delta_e}^{\mathrm{T}}\dot{\bar{E}}_{\delta_e} \\
=\ & -k_V S_V \mathrm{sat}(S_V) - k_h S_h \mathrm{sat}(S_h) + [S_V, S_h] \begin{bmatrix} b_{11} & b_{12} \\ b_{21} & b_{22} \end{bmatrix} \begin{bmatrix} \hat{\beta}_{\mathrm{cf}} + \beta_{\mathrm{cn}} - \beta_c^* \\ \hat{\delta}_{\mathrm{ef}} + \delta_{\mathrm{en}} - \delta_e^* \end{bmatrix} + \frac{1}{\eta_1}\bar{A}_{\beta_c}^{\mathrm{T}}\dot{\bar{A}}_{\beta_c} + \frac{1}{\eta_2}\bar{A}_{\delta_e}^{\mathrm{T}}\dot{\bar{A}}_{\delta_e} \\
& + \frac{1}{\eta_3}\left(\hat{E}_{\beta_c} - E_{\beta_c}\right)\dot{\bar{E}}_{\beta_c} + \frac{1}{\eta_4}\left(\hat{E}_{\delta_e} - E_{\delta_e}\right)\dot{\bar{E}}_{\delta_e} \\
=\ & -k_V S_V \mathrm{sat}(S_V) - k_h S_h \mathrm{sat}(S_h) + \bar{A}_{\beta_c}^{\mathrm{T}}\left[\left(S_V b_{11} + S_h b_{21}\right)\xi + \frac{1}{\eta_1}\dot{\bar{A}}_{\beta_c}\right] \\
& + \bar{A}_{\delta_e}^{\mathrm{T}}\left[\left(S_V b_{12} + S_h b_{22}\right)\xi + \frac{1}{\eta_2}\dot{\bar{A}}_{\delta_e}\right] + \left(S_V b_{11} + S_h b_{21}\right)\left(\beta_{\mathrm{cn}} - \varepsilon_{\beta_c}\right) \\
& + \left(S_V b_{12} + S_h b_{22}\right)\left(\delta_{\mathrm{en}} - \varepsilon_{\delta_e}\right) + \frac{1}{\eta_3}\left(\hat{E}_{\beta_c} - E_{\beta_c}\right)\dot{\bar{E}}_{\beta_c} + \frac{1}{\eta_4}\left(\hat{E}_{\delta_e} - E_{\delta_e}\right)\dot{\bar{E}}_{\delta_e}.
\end{aligned} \tag{56}$$

For keeping the system stable, Eq. (56) is required to satisfy $\dot{V} \leqslant 0$. Accordingly, the adaptive laws are designed as follows.

$$\dot{\bar{A}}_{\beta_c} = \dot{\hat{A}}_{\beta_c} = -\eta_1(S_V b_{11} + S_h b_{21})\xi, \tag{57}$$

$$\dot{\bar{A}}_{\delta_e} = \dot{\hat{A}}_{\delta_e} = -\eta_2(S_V b_{12} + S_h b_{22})\xi, \tag{58}$$

$$\dot{\bar{E}}_{\beta_c} = \eta_3 \left|S_V b_{11} + S_h b_{21}\right|, \tag{59}$$

$$\dot{\bar{E}}_{\delta_e} = \eta_4 \left|S_V b_{12} + S_h b_{22}\right|, \tag{60}$$

$$\beta_{\mathrm{cn}} = -\hat{E}_{\beta_c}\mathrm{sgn}(S_V b_{11} + S_h b_{21}), \tag{61}$$

$$\delta_{\mathrm{en}} = -\hat{E}_{\delta_e}\mathrm{sgn}(S_V b_{12} + S_h b_{22}). \tag{62}$$

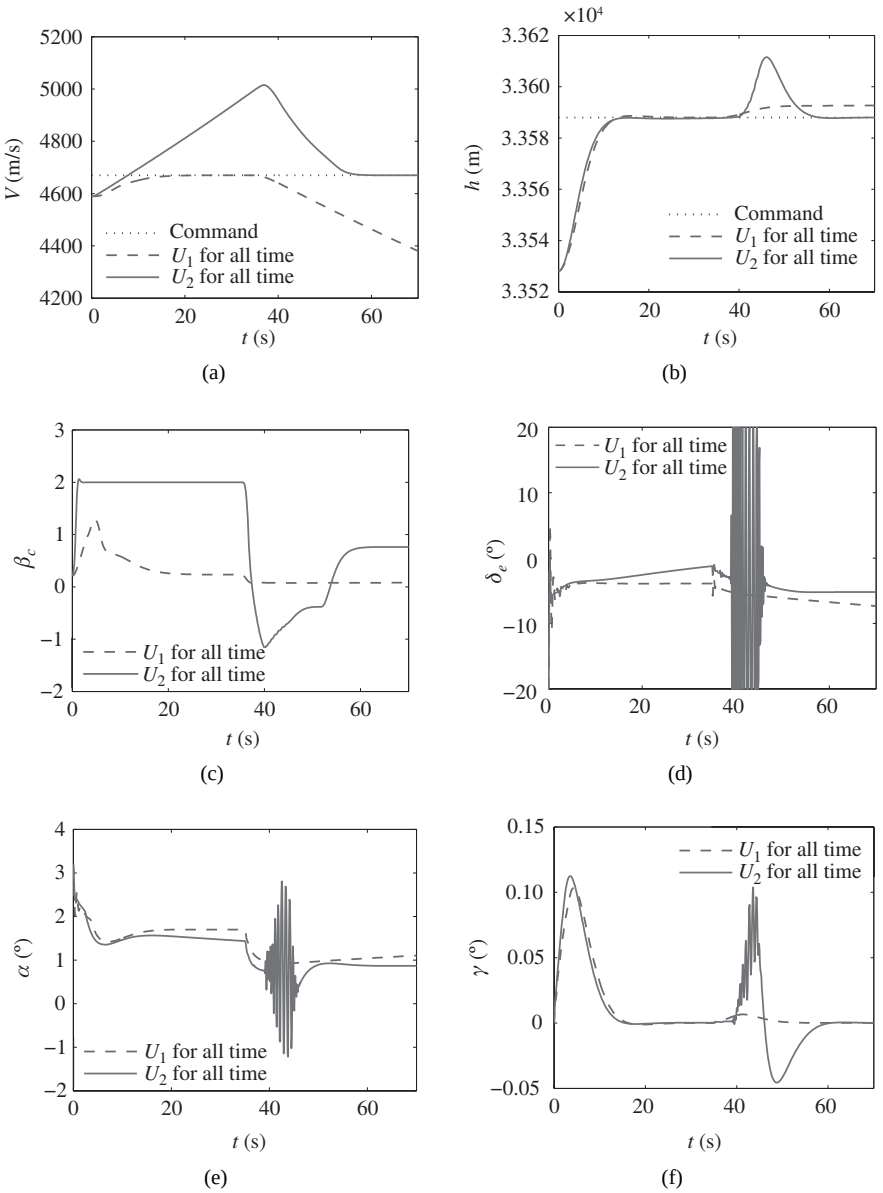

Figure 6 Simulation results of whole process by using U_1 and U_2 for full time respectively. (a) Velocity; (b) altitude; (c) throttle setting; (d) elevator deflection; (e) angle of attack; (f) flight path angle.

From (57)–(62), Eq. (56) can be rewritten as

$$\begin{aligned}\dot{V} &= -k_V S_V \mathrm{sat}(S_V) - k_h S_h \mathrm{sat}(S_h) - \varepsilon_{\beta_c}\left(S_V b_{11} + S_h b_{21}\right) - E_{\beta_c}\left|S_V b_{11} + S_h b_{21}\right| \\ &\quad -\varepsilon_{\delta_e}\left(S_V b_{12} + S_h b_{22}\right) - E_{\delta_e}\left|S_V b_{12} + S_h b_{22}\right| \\ &\leqslant -k_V S_V \mathrm{sat}(S_V) - k_h S_h \mathrm{sat}(S_h) + \left|\varepsilon_{\beta_c}\right|\left|S_V b_{11} + S_h b_{21}\right| - E_{\beta_c}\left|S_V b_{11} + S_h b_{21}\right| \\ &\quad + \left|\varepsilon_{\delta_e}\right|\left|S_V b_{12} + S_h b_{22}\right| - E_{\delta_e}\left|S_V b_{12} + S_h b_{22}\right| \\ &= -k_V S_V \mathrm{sat}(S_V) - k_h S_h \mathrm{sat}(S_h) + \left(\left|\varepsilon_{\beta_c}\right| - E_{\beta_c}\right)\left|S_V b_{11} + S_h b_{21}\right| + \left(\left|\varepsilon_{\delta_e}\right| - E_{\delta_e}\right)\left|S_V b_{12} + S_h b_{22}\right| \\ &\leqslant -k_V S_V \mathrm{sat}(S_V) - k_h S_h \mathrm{sat}(S_h) \leqslant 0. \end{aligned} \tag{63}$$

Hence we establish stability with the adaptive law selection in (57)–(62).

In order to overcome the well-known chattering phenomenon of SMC, the sign function is replaced

Table 1 The membership function parameters of β_{c1} and β_{c2}

Negative			Zero			Positive		
m_{N1}	m_{N2}	σ_N	m_{Z1}	m_{Z2}	σ_Z	m_{P1}	m_{P2}	σ_P
−0.080	0.080	0.272	0.920	1.080	0.272	1.920	2.080	0.272

Table 2 The membership function parameters of δ_{e1} and δ_{e2}

Negative			Zero			Positive		
m_{N1}	m_{N2}	σ_N	m_{Z1}	m_{Z2}	σ_Z	m_{P1}	m_{P2}	σ_P
−0.377	−0.321	0.095	−0.028	0.028	0.095	0.321	0.377	0.095

with the saturation function:

$$\mathrm{sat}(A/k) = \begin{cases} A/k, & \text{if } |A/k| \leqslant 1, \\ \mathrm{sign}(A/k), & \text{otherwise.} \end{cases} \tag{64}$$

This leads to replacement of (61) and (62) with the following:

$$\beta_{\mathrm{cn}} = -\hat{E}_{\beta_c}\mathrm{sat}(S_V b_{11} + S_h b_{21}), \tag{65}$$

$$\delta_{\mathrm{en}} = -\hat{E}_{\delta_e}\mathrm{sat}(S_V b_{12} + S_h b_{22}). \tag{66}$$

Note that the issue for either knowing/measuring/estimating b_{ij} on-line or bypassing the effect of b_{ij} terms in the constructive analysis can be solved by modifying the Lyapunov function (55) to implement the adaptive laws (57)–(62). The authors are working on a further enhancement of the proposed scheme to address this point.

4 Simulation example

U_1 is the control signal in retracting mode, U_2 is the control signal in stretching mode. At first, we use U_1 and U_2 for full time to control the whole process. The simulation results are shown in Figure 6.

From Figure 6, we can see that U_1 cannot control the stretching mode and U_2 cannot control the retracting mode. Therefore, we need to use appropriate method to switch the control signal from U_1 to U_2.

In this paper, we proposed a novel scheme of type-2 TSK fuzzy SMC to realize adaptive control of mode switching for HMA. The initial parameters of membership functions for type-2 TSK fuzzy SMC are shown in Tables 1 and 2.

In Tables 1 and 2, the linguistic variables 'Negative', 'Zero', and 'Positive' are what we defined to represent the labels of membership function. m_{N1}, m_{N2} are the means of membership function of type-2 fuzzy subset 'Negative', $m_{N1} \leqslant m_{N2}$, and σ_N is the variance of type-2 fuzzy subset 'Negative'; m_{Z1}, m_{Z2} are the means of membership function of type-2 fuzzy subset 'Zero', $m_{Z1} \leqslant m_{Z2}$, and σ_Z is the variance of type-2 fuzzy subset 'Zero'; m_{P1}, m_{P2} are the means of membership function of type-2 fuzzy subset 'Positive', $m_{P1} \leqslant m_{P2}$, and σ_P is the variance of type-2 fuzzy subset 'Positive'.

According to the membership function parameters shown in Tables 1 and 2 and the adaptive switching signals obtained from (57)–(62) and (65), (66), comparing with the using U_1, U_2, $0.5U_1 + 0.5U_2$, type-1 TSK fuzzy, general smoother method (GSM) [30] which has the same format with (13), respectively. We conduct simulation experiments discussing the control effects of mode switching from winglets retracting mode to winglets stretching mode in 35–40 s. The simulation results are shown in Figure 7.

From the simulation results shown in Figure 7, we can draw the conclusion that when the winglets mode is switched from retracting mode to stretching mode in 35–40 s, comparing with the other five methods, the velocity and altitude of the proposed method can maintain good track performance, without the phenomenon of state saltation. Specially, the velocity of proposed method can switch smoothly from

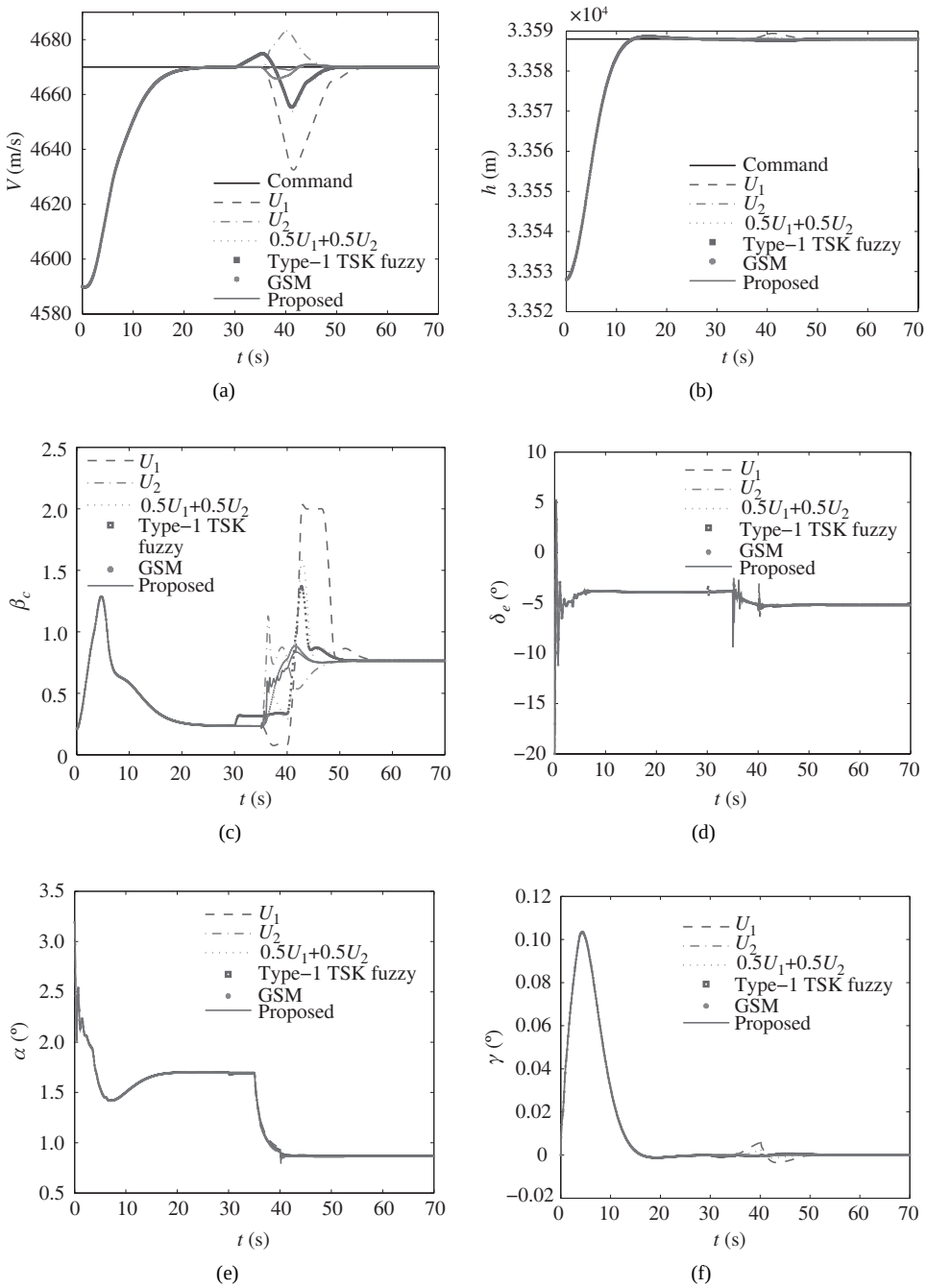

Figure 7 Simulation results of whole process by using different methods (note that mode switching is in 35–40 s). (a) Velocity; (b) altitude; (c) throttle setting; (d) elevator deflection; (e) angle of attack; (f) flight path angle.

35 s, comparing that the velocity of other methods have certain track errors. Furthermore, the other states of proposed method are also switched smoother than the states of other five methods, which illustrate that the proposed method has better effects of mode switching for the HMA. For the type-2 TSK fuzzy, the fuzzy sets are also fuzzy, which is more suitable to deal with uncertain problems. In this paper, we draw upon type-2 TSK fuzzy to distribute the uncertain weights of control signals in retracting and stretching modes respectively. In theory, the basic type-1 TSK fuzzy design can fulfill the task, but the effects are unsatisfactory. There are two reasons. First, the fuzzy sets need to be set and they cannot be changed; while in this paper, the fuzzy sets can be adaptive adjusted according to the flight states. Second, the membership functions of fuzzy sets of basic type-1 TSK fuzzy are certain, while the

membership functions of fuzzy sets of type-2 TSK fuzzy have uncertain means, which are more suitable to deal with uncertain problems.

5 Conclusion

This paper has presented a novel adaptive control of mode switching for HMA based on type-2 TSK fuzzy SMC, in order to maintain stability and smoothness in the switching process of retracted winglets. First, the model of HMA and the aerodynamic parameters in retracting mode, stretching mode and switching mode respectively are given. Then, the switching mechanism is discussed that SMC is used in retracting mode and stretching mode respectively, and the adaptive control of mode switching is used in switching process. Furthermore, The combination of type-2 TSK fuzzy and SMC is designed for the switching process considering that the format of control of mode switching is similar to the type-2 TSK fuzzy. Afterwards, in order to keep robustness of flight control system and smoothness of mode switching process, a direct constructive Lyapunov analysis is adopted and the adaptive laws are produced correspondingly. Finally, two simulation experiments conducted and compared demonstrate that the combined adaptive control of mode switching based on type-2 TSK fuzzy SMC has good tracking performance.

Acknowledgements

This work was supported by National Natural Science Foundation of China (Grant No. 61304223), Funding of Jiangsu Innovation Program for Graduate Education (Grant No. CXZZ13_0170), Funding for Outstanding Doctoral Dissertation in NUAA (Grant No. BCXJ13-06), and Fundamental Research Funds for the Central Universities.

References

1 Xu B, Shi Z K. An Overview on flight dynamics and control approaches for hypersonic vehicles. Sci China Inf Sci, 2015, 58: 070201
2 Wang Q, Stengel R F. Robust nonlinear control of a hypersonic aircraft. J Guid Control Dyn, 2000, 23: 577–585
3 Xu H J, Mirmirani M D, Ioannou P A. Adaptive sliding mode control design for a hypersonic flight vehicle. J Guid Control Dyn, 2004, 27: 829–838
4 Guo C, Liang X G, Wang J W. Multi-model soft switching tracking control and robust least-squares weighted control allocation for near space interceptor. In: Proceedings of the 33rd Chinese Control Conference, Nanjing, 2014. 4210–4215
5 Chen M, Wu Q, Jiang C, et al. Guaranteed transient performance based control with input saturation for near space vehicles. Sci China Inf Sci, 2014, 57: 052204
6 Xu B, Gao D, Wang S. Adaptive neural control based on HGO for hypersonic flight vehicles. Sci China Inf Sci, 2011, 54: 511–520
7 Xu B. Robust adaptive neural control of flexible hypersonic flight vehicle with dead-zone input nonlinearity. Nonlinear Dyn, 2015, 80: 1509–1520
8 Xu B, Huang X, Wang D, et al. Dynamic surface control of constrained hypersonic flight models with parameter estimation and actuator compensation. Asian J Control, 2014, 16: 162–174
9 Huang Y, Sun C, Qian C, et al. Non-fragile switching tracking control for a flexible air-breathing hypersonic vehicle based on polytopic LPV model. Chin J Aeronaut, 2013, 26: 948–959
10 Zhang R, Sun C, Zhang J, et al. Second-order terminal sliding mode control for hypersonic vehicle in cruising flight with sliding mode disturbance observer. J Control Theory Appl, 2013, 11: 299–305
11 Zhang R, Wang L, Zhou Y. On-line RNN compensated second order nonsingular terminal sliding mode control for hypersonic vehivle. Int J Intel Comput Cybern, 2012, 5: 186–205
12 Wang J, Zone Q, Su R, et al. Continuous high order sliding mode controller design for a flexible air-breathing hypersonic vehicle. ISA Trans, 2014, 53: 690–698
13 Zong Q, Wang J, Tian B, et al. Quasi-continuous High-order sliding mode controller and observer design for flexible hypersonic vehicle. Aerosp Sci Technol, 2013, 27: 127–137
14 Taheri B, Case D, Richer E. Force and stiffness backstepping-sliding mode controller for pneumatic cylinders. IEEE/ASME Trans Mechatron, 2014, 19: 1799–1809
15 Ren Q, Balazinski M, Baron L. Type-2 TSK fuzzy logic system and its type-1 counterpart. Int J Comput Appl, 2011, 20: 8–13

16 Zheng G, Wang J, Jiang L. Research on type-2 TSK fuzzy logic systems. Fuzzy Info Eng, 2009, 2: 491–500
17 Biglarbegian M, Melek W W, Mendel M J. On the stability of interval type-2 TSK fuzzy logic control systems. IEEE Trans Syst Man Cybern Part B-Cybern, 2010, 40: 798–818
18 Boumella N, Djouanim K, Boulemden M. A robust interval type-2 TSK fuzzy logic system design based on chebyshev fitting. Int J Control Autom Syst, 2012, 10: 727–736
19 Takagi T, Sugeno M. Fuzzy identification of systems and its applications to modeling and control. IEEE Trans Syst Man Cybern, 1985, 15: 116–132
20 Gao D, Sun Z. Fuzzy tracking control design for hypersonic vehicles via T-S model. Sci China Inf Sci, 2011, 54: 521–528
21 Gao D, Sun Z, Du T. Dynamic surface control for hypersonic aircraft using fuzzy logic system. In: Proceedings of IEEE International Conference on Automation and Logistics, Jinan, 2007. 2314–2319
22 Li H, Pan Y, Yu Z, et al. Fuzzy output-feedback control for non-linear systems with input time-varying delay. IET Control Theory Appl, 2014, 8: 738–745
23 Jafarzadeh S, Fadali M S. On the Stability and control of continuous-time TSK fuzzy systems. IEEE Trans Cybern, 2013, 43: 1073–1087
24 Saltzman J E, Wang K C, Iliff W K. In-flight subsonic lift and drag characteristics unique to blunt-based lifting reentry vehicles. AIAA J Spacecraft Rocket, 2007, 44: 299–309
25 Shaughnessy J D, Pinckney S Z, Mcminn J D, et al. Hypersonic vehicle simulation model: winged-cone configuration. NASA Langley Research Center, 1990
26 Hwang J H, Kwak H J, Park G T. Adaptive interval type-2 fuzzy sliding mode control for unknown chaotic system. Nonlinear Dyn, 2011, 63: 491–502
27 Mendel M J. General type-2 fuzzy logic systems made simple: a tutorial. IEEE Trans Fuzzy Syst, 2014, 22: 1162–1182
28 Wu D. Approaches for reducing the computational cost of interval type-2 fuzzy logic systems: overview and comparisons. IEEE Trans Fuzzy Syst, 2013, 21: 80–93
29 Mendel M J. Uncertain Rule-based Fuzzy Logic Systems: Introduction and New Directions. Upper Saddle River: Prentice Hall, 2001
30 Dou G H, Gao Z H. Simulation and design of fade-out devices. Sci Technol Eng, 2012, 12: 1671–1815